

Effects of Organoclay Modification on Microstructure and Properties of Polypropylene–Organoclay Nanocomposites

Jin Woo Lee,* Mun Ho Kim, Won Mook Choi, O Ok Park

Department of Chemical and Biomolecular Engineering, Korea Advanced Institute of Science and Technology, 373-1 Guseong-dong, Yuseong-gu 305-701, Republic of Korea

Received 24 February 2005; accepted 27 May 2005

DOI 10.1002/app.22704

Published online in Wiley InterScience (www.interscience.wiley.com).

ABSTRACT: We prepared polypropylene nanocomposites based on a modified organoclay with isobutyl trimethoxysilane to investigate the effects of such modifications of organoclay on the microstructure and properties of the nanocomposite. The organoclay was preliminarily intercalated with distearyldimethylammonium bromide via an ion exchange before being grafted with silane. The morphology of the polypropylene–organoclay nanocomposites was characterized by wide-angle X-ray diffraction analyses and transmission electron microscopy. The modification of the edges of clay platelets with organic silane resulted in a more uniform dispersion of nonagglomerated tactoids, which con-

sisted of several intercalated clay platelets. However, the unmodified organoclay led to a mixed morphology with both agglomerated and nonagglomerated tactoids. The grafting of the clay edges with organic silane also affected the linear viscoelastic properties of the nanocomposites in the melt state, which was shown to be sensitive to the interaction between the edges of clay platelets as well as to the interaction of the polymer with the platelet edges. © 2005 Wiley Periodicals, Inc. *J Appl Polym Sci* 99: 1752–1759, 2006

Key words: clay; modification; polypropylene; nanocomposite; interface

INTRODUCTION

In the past 20 years there has been increased interest in the synthesis of nanocomposite materials by dispersing nanosized inorganic particles into polymers.¹ Among a wide range of nanostructured materials, much effort has recently focused on the elaboration of polymer-layered silicate nanocomposites using natural and synthetic clay minerals because of the remarkable improvement of various material properties.² Clay minerals such as montmorillonite (MMT) exhibit many interesting structural features including exchangeable interlayer cations, hydroxyl groups on the edges of clay platelets, and a high aspect ratio and small dimensions of the individual layers. However, the pristine silicate surface is generally too hydrophilic to be compatible with most polymers. To render the clay surface hydrophobic, they are intercalated with organic cations such as alkylammonium salt by an ion exchange.³

The grafting with organic silane on the hydroxyl groups present on the edge of clay platelets is another way to modify the clay.^{4–7} The hydroxyl edges of clay

platelets could possibly enhance the attractive interaction with a polar polymer, but they could have an adverse effect on the intercalation of a nonpolar polymer such as polyolefin.⁸ Recently, Zhao et al. reported that the intercalated structure in a polyethylene (PE)–clay nanocomposite could be formed without a compatibilizer, such as maleic anhydride (MA) grafted PE, using a modified organoclay with trimethylchlorosilane.⁵ In their study, the clay was first grafted with trimethylchlorosilane and then the modified clay was intercalated with an alkylammonium cation. In general, the intercalation of hydrophobic PE chains into the clay interlayer can hardly occur without a polar compatibilizer. They attributed such improvement of the clay dispersion to the enhanced wetting ability between PE and organoclay that was due to the grafting with silane.

Polypropylene (PP) is one of the most widely used polyolefins. Since the successful preparation of PP–clay nanocomposites with MA grafted PP (PP-g-MA) as a compatibilizer,⁹ various studies on the preparation and characterization of PP–clay nanocomposites have been reported.^{10,11} PP-g-MA is known to facilitate the dispersion of clay particles in a nonpolar PP matrix and to increase the adhesion between PP and the clay particle.¹⁰

In this work, we report the preparation of a PP nanocomposite based on a modified organoclay with isobutyl trimethoxysilane. We examine the effects of such a modification of organoclay on the microstruc-

*Present address: Performance Polymers R&D, Research Park, LG Chem, Ltd., 104-1, Moonji-dong, Yuseong-gu, Daejeon 305-380, Republic of Korea.

Correspondence to: O. O. Park (ookpark@kaist.ac.kr).

ture, mechanical properties, and linear viscoelastic properties of PP-organoclay nanocomposites. Before grafting with silane, the organoclay is preliminarily intercalated with alkylammonium ions via ion exchange. We use PP-g-MA as a compatibilizer to enhance the degree of clay dispersion in the PP matrix. These results are interpreted in terms of the interaction between the dispersed clay platelets and in terms of the interaction of the polymer with dispersed clay. Finally, the plausible mechanism of clay dispersion is proposed.

EXPERIMENTAL

Materials

The matrix materials used here are PP from Honam Petrochemical [weight-average molecular weight (M_w) = 230,000 g/mol from gel permeation chromatography] and PP-g-MA from Uniroyal Chemical (M_w = 210,000 g/mol from gel permeation chromatography, MA content = 0.5 wt %). Sodium MMT (Na-MMT) with a cation exchange capacity (CEC) of about 95 mequiv/100 g was obtained from Southern Clay Products, Inc. Distearylidimethyl ammonium bromide (Tokyo Chemical Industry) was used as received. Isobutyl trimethoxysilane and diethylamine were purchased from Aldrich Chemical.

Preparation of organoclay

Organoclay was synthesized by a cation exchange reaction between Na-MMT and excess alkylammonium salt (1.5 times the exchange capacity of the host). The alkylammonium cation was dissolved in a 50 : 50 (v/v) mixture of ethanol and deionized water at approximately 65°C. The clay particles (1 wt %) were preliminarily dispersed in a 50 : 50 (v/v) mixture of ethanol and deionized water by using a homogenizer. The alkylammonium solution was added to the suspension of the clay particles, and the mixture was then stirred vigorously by using a homogenizer for 40 min at approximately 65°C. The cation-exchanged clay particles were collected by filtration and subsequently washed 4 times with a 50 : 50 (v/v) mixture of hot ethanol and deionized water. An AgNO₃ test confirmed the absence of halide anions. The filter cake was dried at room temperature, ground, and further dried at 85°C under a vacuum for at least 24 h.

Grafting of organic silane onto organoclay

Organoclay (5 g) was placed in a 500-mL round-bottomed flask containing 200 mL of dry toluene under a nitrogen flow. The required amount of an organic silane (3.4 mL) was added with the diethylamine (1.6 mL) as a catalyst to the stirred suspension. The mix-

ture was then stirred at 40°C for 20 h under a flow of dry nitrogen. The modified organoclay was washed 3 times with dry toluene, followed by methanol and acetone washings using centrifugation. The modified organoclay was dried in a vacuum oven at room temperature and then at 85°C for at least 24 h. The interlayer spacing of the modified organoclay was measured by wide-angle X-ray diffraction (WAXD) analysis. For evaluation of the silane content, the extraction of alkylammonium ions was performed.¹² A small portion of the modified organoclay was placed in excess (350 mL/g) acidified ethanol (0.2M HCl) and refluxed for 4 h. The products were recovered by suction filtration, washed with ethanol, and dried under a vacuum at 90°C for at least 24 h. The extraction procedure was repeated twice. The elemental analyses were performed for both the extracted and nonextracted types of the modified organoclay by using an EA1110-FISONs elemental analyzer. The bare MMT or Na-MMT was also characterized for comparison. The grafted amount of silane molecules (mequiv grafted silane/100 g bare MMT) was calculated using the following equation^{4,13}:

$$\text{grafted amount (mequiv/100 g)} = \frac{10^5 \Delta C}{(1200N_C - \Delta C(M - 1))} \quad (1)$$

where N_C and M (g/mol) designate the number of carbon atoms and the molecular weight of the grafted silane molecule, respectively ($N_C = 4$, $M = 133.2$), and ΔC is the difference between the carbon content of Na-MMT and the carbon content of the extracted modified organoclay with trialkoxysilane (S-OMMT).

Preparation of PP/clay nanocomposites

The mixture of dried pellets of PP and PP-g-MA and the dry powder of sieved organoclay (<50 μm) was compounded by using an internal mixer (Brabender plastograph) for 10 min at 180°C (measured by an internal thermocouple) with a screw speed of 50 rpm. The inorganic contents of clay in the nanocomposites were taken as the values reported at 600°C by thermogravimetric analyses for the compounded materials. Thermogravimetric analysis was performed under air on a Dupont Instruments TA 2200 with a heating ramp of 20°C/min from room temperature to 900°C.

WAXD analysis

WAXD was conducted at ambient temperature on a Rigaku D/MAX-RC diffractometer with Cu K α radiation at a wavelength of 1.5406 Å. The organoclays were studied as powders. The compounded materials were prepared in thin films by compression molding

TABLE I
Characteristics of Clays Used in Study

Abbreviation	Organic modifier		d_{001} (nm) ^a
	Organic ion	Organic silane	
Na-MMT	None	None	1.20
OMMT	Dimethyldistearylammonium chloride	None	2.67
S-OMMT	Dimethyldistearylammonium chloride	Isobutyltrimethoxy silane	2.66

^a The (001) basal spacing was determined from XRD measurements.

for WAXD analysis. Each sample was scanned from 2θ 1.2° to 10° at a scan rate of $1^\circ/\text{min}$.

Rheological characterization

Rheological measurements were conducted on a controlled strain rheometer (ARES, Rheometric Scientific) with 25-mm diameter parallel plates in a nitrogen environment. Linear viscoelastic measurements were performed over a frequency range of 0.05–300 rad/s at 190°C . Sample disks were prepared by compression molding at 190°C . The thickness of a typical sample ranged from 0.7 to 0.8 mm. For all measurements the samples were equilibrated in the rheometer after loading for 30 min prior to testing. During this period, the dynamic storage modulus was monitored at a frequency of 1 rad/s. After 30 min, no significant change was observed.

Mechanical measurement

The compounded materials were injection molded into dogbone-shaped tensile bars by using a mini-molder (Bau-tech). The cylinder temperature was kept at 215°C and the molds were heated to 50°C . The tensile tests were conducted according to ASTM D 638 at room temperature by using a tensile testing machine. The crosshead speed was 5 mm/min. At least five runs were performed for each specimen. The tensile elongation was over 300% for every specimen.

Differential scanning calorimetry

The degree of crystallinity (X_c) was evaluated by differential scanning calorimetry (Q-100, TA Instruments). The samples were first heated to 200°C under nitrogen and held for 5 min to erase the thermal history. These samples were then cooled at different cooling rates and heated again to 200°C . We calculated the X_c from the heat of fusion (ΔH_f) on the second heating as follows:

$$X_c = \frac{\Delta H_f}{\Delta H_0(1 - \Phi_{\text{clay}})} \quad (2)$$

where ΔH_0 designates the melting enthalpy of 100% crystalline PP ($\Delta H_0 = 208 \text{ J/g}$)¹⁴ and Φ_{clay} indicates the fraction of organoclay in the nanocomposite.

Transmission electron micrographs

The degree of clay dispersion in the polymer matrix was checked by using a transmission electron microscope (EM 912 Omega, Carl Zeiss) operating at an accelerating voltage of 100 kV. The injection-molded specimens were sectioned into roughly 70-nm thin films for transmission electron microscopy (TEM) observation using a Reichert ultramicrotome.

RESULTS AND DISCUSSION

Modification of organoclay

MMT is generally described as being made of nano-sized and disk-shaped crystalline lamellae. The edge of the disk is similar to a hydrous oxide and is characterized by the presence of hydroxyl groups. MMT also contains intralayer AlOH groups, but these groups are believed to be hardly accessible to the coupling agent molecules such as alkoxy silane because of the size of the molecules.¹⁵ Therefore, only the edge hydroxyl sites can probably react with the silane molecules. It has been reported that liophilized clay, such as Na-MMT intercalated with alkylammonium ions, can readily disperse into toluene.¹⁶ In our system, we also obtained a slightly brown but nearly transparent suspension when organoclay was suspended in toluene. The following reports the chemical modification of the organoclay in toluene using trialkoxy silane.

We modified the organoclay with isobutyl trimethoxysilane. For the grafting we used the organoclay that had already been intercalated with alkylammonium ions (OMMT). Table I shows that the interlayer spacing of the S-OMMT has nearly the same value as that of OMMT. The grafting of silane occurs on the edge hydroxyl sites, which explains why there is little change in the interlayer spacing. To gain the evidence of the reaction and the quantitative data, we performed the extraction of alkylammonium ions for S-OMMT. Table II shows the results of the elemental

TABLE II
Elemental Analyses of Na-MMT and Extracted S-OMMT

Samples	Nitrogen content (wt %)	Carbon content (wt %)	ΔC (%) ^a	Grafted amount (mequiv/100 g) ^b
Na-MMT	0.02	1.10	—	—
S-OMMT	0.03 (0.91) ^c	3.30 (27.15) ^c	2.20	0.48

^a The difference in the carbon content between Na-MMT and the extracted S-OMMT.

^b Determined using eq. (1).

^c The nitrogen or carbon content of S-OMMT before extraction of alkylammonium ions.

analyses for the extracted and nonextracted types of S-OMMT. After extraction, the nitrogen content of S-OMMT decreased to almost zero, which is almost the same value as that of bare Na-MMT. This result indicates that the alkylammonium ions were completely removed by extraction. In contrast, the remaining carbon content is greater in the extracted S-OMMT than in the bare Na-MMT, thereby confirming the presence of silane molecules that have been covalently bonded on the clay platelets. The grafted amount of silane molecules was calculated from eq. (1), which was about 48 mequiv/100 g. Considering that the CEC of Na-MMT is 95 mequiv/100 g, we posit that a substantial amount of silane molecules exist on the edges of clay platelets and that this amount corresponds to roughly half the amount of alkylammonium molecules intercalated into Na-MMT.

Morphology and mechanical properties of PP-organoclay nanocomposites

We prepared the PP-organoclay nanocomposites by melt mixing, and the compositions of the nanocomposites are listed in Table III. In Figure 1 we see that PP-OMMT nanocomposites (PPNC-OMMT), as well as PP-S-OMMT nanocomposites (PPNC-S-OMMT), have an apparent peak at approximately 2θ 2.5°. This result implies that a nanocomposite with an intercalated structure was obtained.⁹ No difference between

TABLE III
Compositions and Abbreviations of Polypropylene Nanocomposites

Abbreviation	Clay type	Composition (wt %)		
		PP	PP-g-MA	Inorganic content ^a
PP	—	100	—	—
PP-PP-g-MA	—	80	20	—
PPNC-OMMT	OMMT	76	18	3.89
PPNC-S-OMMT	S-OMMT	76	18	3.85

^a Determined from thermogravimetric analyses.

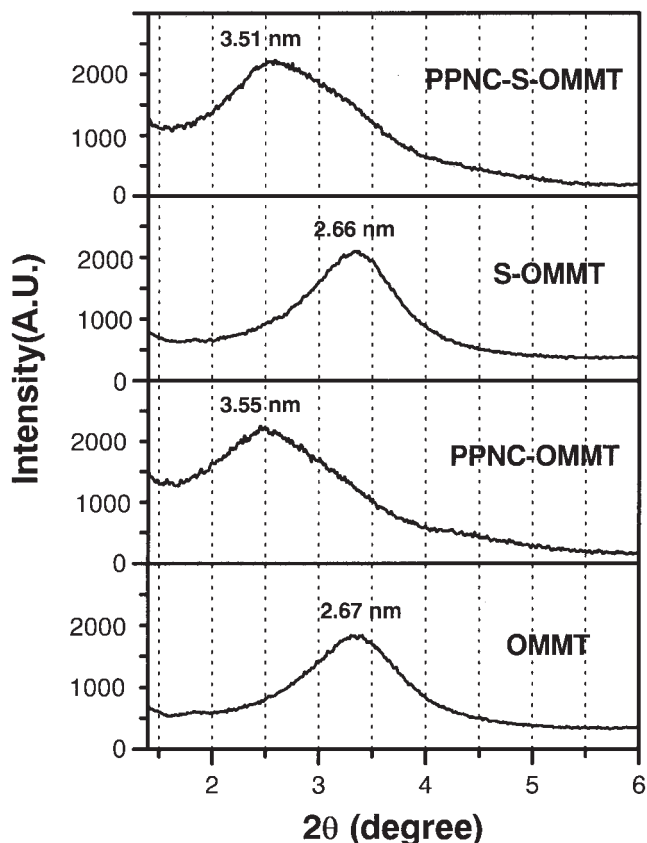
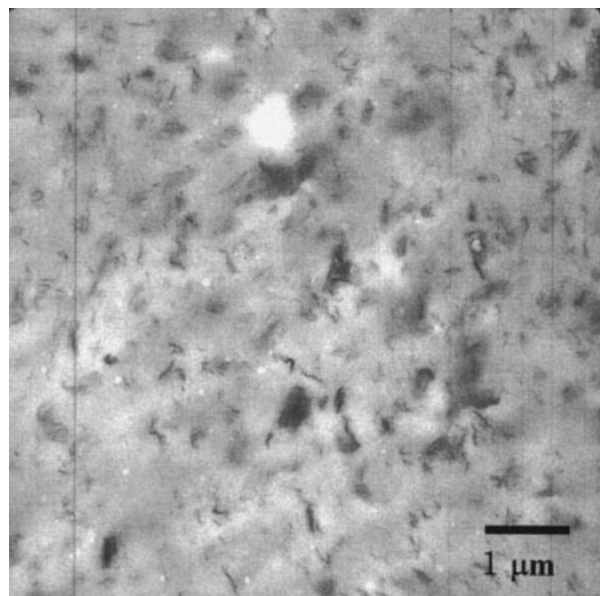


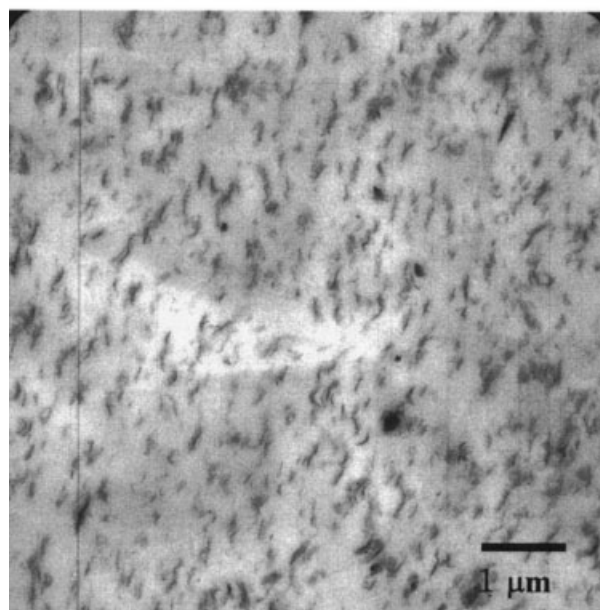
Figure 1 XRD patterns of organoclays and PP nanocomposites.

PPNC-OMMT and PPNC-S-OMMT was observed in the WAXD results. However, WAXD can only detect the periodically stacked layers of the clay particles and little can be said about the spatial distribution of the clay particles. In contrast, TEM observation allowed a qualitative understanding of the microstructure.

The TEM images in Figure 2 clearly show the difference in the clay dispersion between PPNC-OMMT and PPNC-S-OMMT, which was not found in the WAXD patterns. The image for PPNC-S-OMMT appears to have a higher density of tactoids, which consist of several intercalated silicate layers; the image also shows a more uniform dispersion of the nonagglomerated tactoids [Fig. 2(b)]. However, the image for PPNC-OMMT shows a mixed morphology with both agglomerated and nonagglomerated tactoids [Fig. 2(a)]. At higher magnification, the TEM image for PPNC-OMMT shows this agglomeration of tactoids more clearly [Fig. 3(a)]. By contrast, we can observe the fine dispersion of intercalated platelets and some individual layers for PPNC-S-OMMT [Fig. 3(b)]. This difference is also apparent in the tensile properties of the two nanocomposites. As listed in Table IV, the Young's moduli and the tensile strength are higher in PPNC-S-OMMT than in PPNC-OMMT. When the clay particles are dispersed more finely, we can get a



(a)



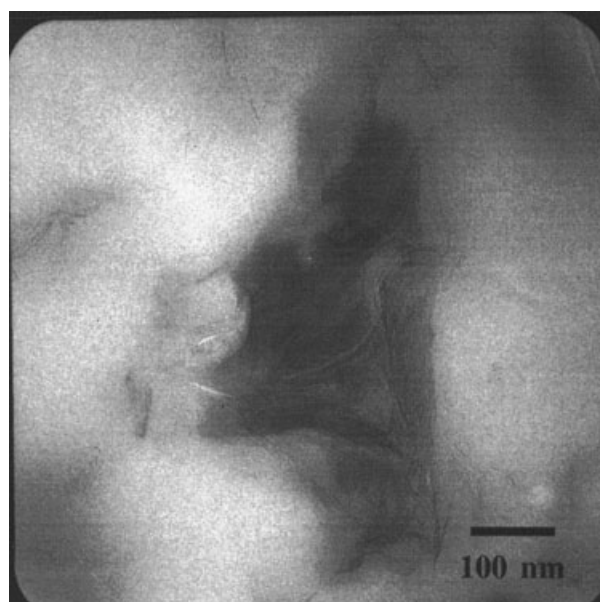
(b)

Figure 2 TEM images of (a) PPNC-OMMT and (b) PPNC-S-OMMT (original magnification $\times 10,000$).

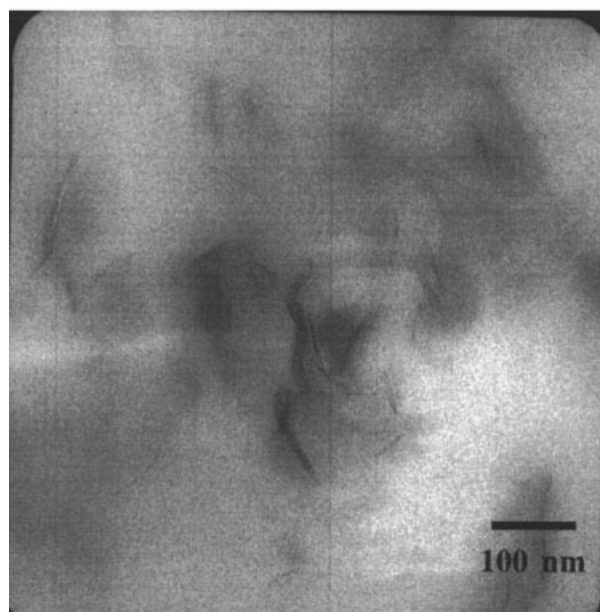
higher aspect ratio of the dispersed particles and a larger interfacial area, both of which make the stress transfer to the silicate layers much more effective; and, in turn, these improvements increase the tensile properties.^{17–19} Considering that the inorganic content and crystallinity of the PPNC-S-OMMT are nearly the same as those of the PPNC-OMMT, the enhanced

reinforcement in PPNC-S-OMMT is thought to result from the improvement in the degree of clay dispersion.

In summary, the modification of clay edges with silane has little effect on the interlayer spacing of organoclay in PP-clay nanocomposites, as seen in the WAXD results. This means that the modification of the



(a)



(b)

Figure 3 TEM images of (a) PPNC-OMMT and (b) PPNC-S-OMMT at higher magnification compared to Figure 2 (original magnification $\times 100,000$).

TABLE IV
Tensile and Thermal Properties of Polypropylene Nanocomposites

Samples	Young's modulus (MPa)	Yield stress (MPa)	Cooling rate (°C/min)	X_c (%) ^a
PP	462 ± 21 (1.01) ^b	39.1 ± 0.16 (0.98) ^b	5 20	52.2 48.4
PP-PP-g-MA	458 ± 10 (1.00)	39.9 ± 0.33 (1.00)	5 20	52.9 48.4
PPNC-OMMT	558 ± 11 (1.22)	42.4 ± 0.41 (1.06)	5 20	52.1 48.7
PPNC-S-OMMT	582 ± 15 (1.27)	43.2 ± 0.18 (1.08)	5 20	51.9 49.4

^a Determined from DSC measurements using eq. (2).

^b The values in the parentheses indicate the relative modulus or stress with respect to the matrix polymer (PP-PP-g-MA).

edge sites does not affect the intercalation capability of PP-g-MA chains into the clay interlayer. However, such modification gives rise to more uniform dispersion of nonagglomerated tactoids compared to the unmodified organoclay, as seen in TEM observations and as confirmed by the results of the tensile tests.

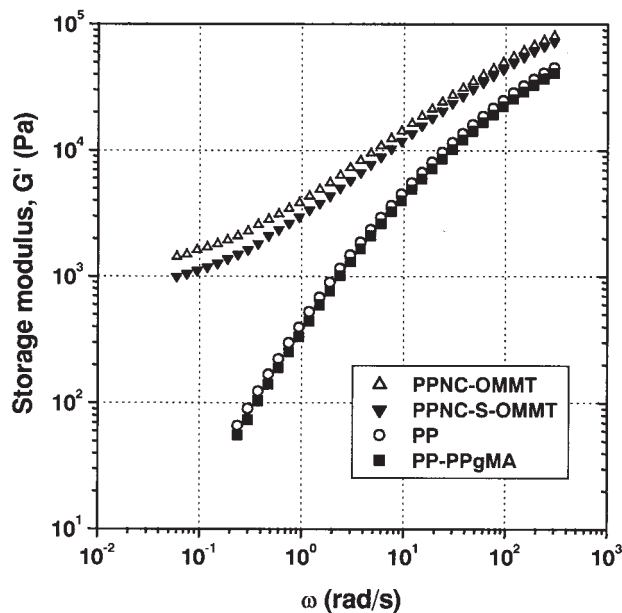
Rheological properties

The linear viscoelastic properties of polymer-clay nanocomposites are known to be very sensitive to the mesoscale dispersion of clay particles and the strength of the polymer-clay interaction.²⁰⁻²³ Figures 4 and 5 show the linear viscoelastic properties of PP, PP-PP-g-MA, and the nanocomposites in the melt state. For both PPNC-S-OMMT and PPNC-OMMT, we can clearly observe the apparent plateau of the storage and loss moduli (Fig. 4) and the diverging of the complex viscosity (Fig. 5) at low frequencies. This pseudosolid-like behavior at low frequencies might be explained in terms of the formation of the percolated structure of the anisotropic tactoids of clay platelets in the quiescent state or in terms of frictional interactions between the anisotropic clay tactoids.^{21,22}

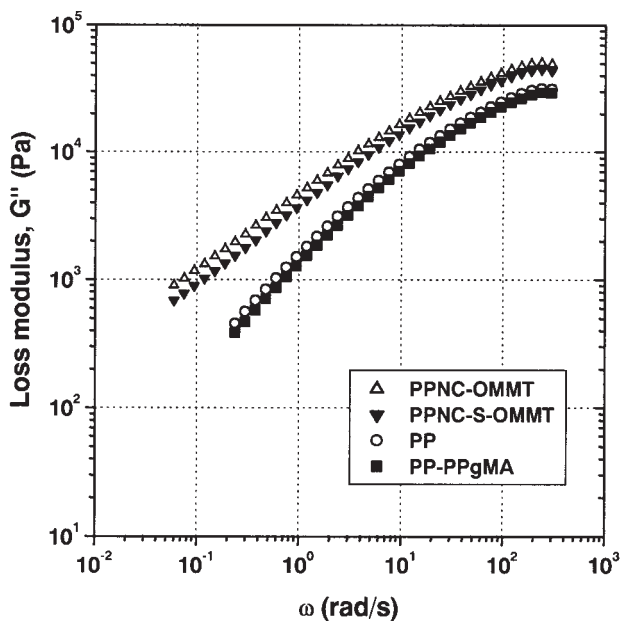
In contrast, the dynamic moduli and the complex viscosity of PPNC-S-OMMT at low frequencies show lower absolute values than those of PPNC-OMMT. In fact, we expected the increases in the dynamic moduli of PPNC-S-OMMT at low frequencies, as well as the increases in the complex viscosity, to be larger than those of PPNC-OMMT, because the fine dispersion of clay particles is thought to give rise to a more retarded relaxation in terms of the frictional interactions between the clay tactoids. This retarded relaxation corresponds to the increases in the storage modulus and the complex viscosity at low frequencies.

To explain this discrepancy, we noted the influence of the edge sites of clay platelets on the pseudosolid-

like behaviors at low frequencies. With respect to the filler-filler interaction in the percolated structure, the hydroxyl groups on the edge of clay platelets could possibly increase the frictional interaction between the clay tactoids in the network via hydrogen bonding or via a polar interaction between the hydroxyl edges. This increase in frictional interaction can contribute to a more retarded relaxation at low frequencies. In addition, the attractive interaction between the polar



(a)



(b)

Figure 4 The (a) storage modulus and (b) loss modulus of PP, PP/PPgMA blend, and PP nanocomposites at 190°C.

edges and functional groups in PP-g-MA may also contribute greatly to the long relaxation. By contrast, the grafting of the edge sites of silicate layers with organic silane is expected to decrease the foregoing interactions substantially. Therefore, we can expect the increases in the dynamic moduli or the complex viscosity to be less pronounced for PPNC-S-OMMT, regardless of the fine dispersion of the clay tactoids.

Possible dispersion mechanism

In the process of clay dispersion, the conversion of pristine clay to an intercalated hybrid requires polymer chains to be transported from the molten bulk into the silicate interlayer.^{24,25} On the basis of the TEM observations, Vaia et al. summarized the morphology of organoclay as follows²⁴: the clay particles are composed of agglomerations of smaller, oblong-shaped particles. These oblong-shaped particles (primary particles) have a lateral dimension from a few 10ths to 10 μm . The primary particles generally consist of a compact face-face stacking or low-angle intergrowth of individual silicate crystallites. For intercalation to occur, the polymer must be transported from the agglomerate-polymer interface to the primary particles and then to the edges of the tactoids.

On the basis of the morphology of organoclay, we can explain how the silane modification of the clay edges affects the dispersion process of clay particles in a polymer matrix. That is, to form an intercalated structure in a PP-organoclay nanocomposite with PP-g-MA as the compatibilizer, the PP-g-MA chains should first intercalate into the clay interlayer in order

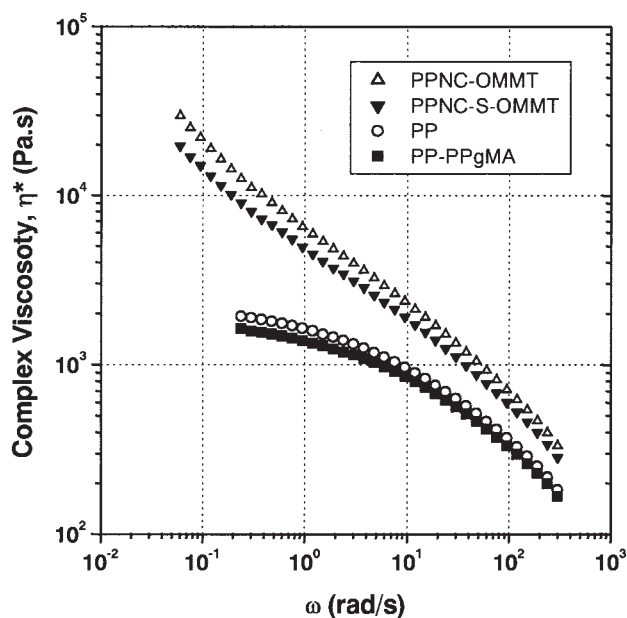


Figure 5 The complex viscosity of PP, PP/PPgMA blend, and PP nanocomposites at 190°C.

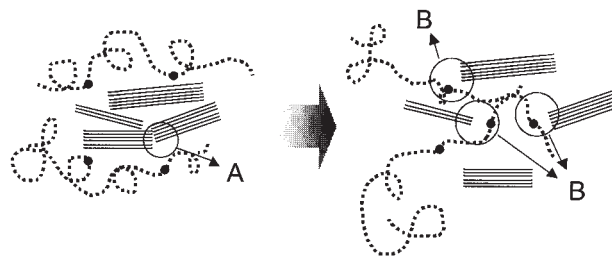


Figure 6 A schematic illustration for the possible interaction between the edges of clay tactoids and between PPgMA chains and the clay edges during melt mixing.

to facilitate the dispersion of intercalated tactoids into the nonpolar PP matrix.⁹ As mentioned, to enable the intercalation, PP-g-MA chains must be transported from the interface between the PP-g-MA and the clay particles to the edges of the silicate tactoids (Fig. 6). Compared with the polar hydroxylated edges of OMMT, the initial attraction between the tactoids of the clay platelets should be much weaker for S-OMMT (point A, Fig. 6) and the reduced attraction can then facilitate the separation of the tactoids. In addition, the absence of hydroxyl groups on the edges can also decrease the attractive interaction between PP-g-MA and the edge sites (point B, Fig. 6). This decrease in the attractive interaction can make the diffusion of PP-g-MA chains easier. All of these effects can contribute to the fine dispersion of nonagglomerated tactoids in PPNC-S-OMMT.

CONCLUSIONS

We examined the role of the edge sites of clay platelets in a clay dispersion during melt mixing of PP-organoclay nanocomposites and investigated the effects of the edge sites on the filler-filler and polymer-filler interactions. The replacing of the hydroxyl edges with nonpolar organic silane reduces the attractive interaction between the edge sites of clay platelets and also the interaction between polar functional groups in PP-g-MA and the platelet edges, resulting in a high level of enhancement of the clay dispersion. This reduction of the attractive interaction also decreases the frictional interactions by clay tactoids in the percolated network structure polymer when exposed at low-frequency dynamic shear in the melt state, thereby leading to the relatively small increase in the storage modulus or complex viscosity at low frequencies, regardless of the enhancement of the clay dispersion.

References

1. Oriakhi, C. O. *J Chem Ed* 2000, 77, 1138.
2. Sinha Ray, S.; Okamoto, M. *Prog Polym Sci* 2003, 28, 1539.

3. Giannelis, E. P.; Krishnamoorti, R. K.; Manias, E. *Adv Polym Sci* 1998, 138, 107.
4. Herrera, N. M.; Letoffe, J.-M.; Putaux, J.-L.; David, L.; Bourgreat, E. *Langmuir* 2004, 20, 1564.
5. Zhao, C.; Feng, M.; Gong, F.; Qin, H.; Yang, M. *J Appl Polym Sci* 2004, 93, 676.
6. Le Pluart, L.; Duchet, J.; Sautereau, H.; Gérard, J. F. *Macromol Symp* 2003, 194, 155.
7. Seçkin, T.; Gültek, A.; İçduygu, M. G.; Önal, Y. *J Appl Polym Sci* 2002, 84, 164.
8. Shi, H.; Lan, T.; Pinnavaia, T. J. *Chem Mater* 1996, 8, 1584.
9. Kawasumi, M.; Hasegawa, N.; Kato, M.; Usuki, A.; Okada, A. *Macromolecules* 1997, 30, 6333.
10. Manias, E.; Touny, A.; Wu, L.; Strawhecker, K.; Lu, B.; Chung, T. C. *Chem Mater* 2001, 13, 3516.
11. Leuteritz, A.; Pospiech, D.; Kretzschmar, B.; Willeke, M.; Jehnichen, D.; Jentzsch, U.; Grundke, K.; Janke, A. *Adv Eng Mater* 2003, 5, 678.
12. Melde, B. J.; Holland, B. T.; Blanford, C. F.; Stein, A. *Chem Mater* 1999, 11, 3302.
13. Berndsen, G. E.; De Galan, R. J. *J Liq Chromatogr* 1978, 1, 561.
14. Moore, Jr., E. P. Ed. *Polypropylene Handbook: Polymerization, Characterization, Properties, Processing, Applications*; Hanser/Gardner: Munich, 1996.
15. Morris, H. D.; Bank, S.; Ellis, P. D. *J Phys Chem B* 1990, 94, 3121.
16. Okamoto, M.; Taguchi, H.; Sato, H.; Kotaka, T.; Tateyama, H. *Langmuir* 2000, 16, 4055.
17. LeBaron, P. C.; Wang, Z.; Pinnavaia, T. J. *Appl Clay Sci* 1999, 15, 11.
18. Jones, R. A. L.; Richards, R. W. *Polymer at Surfaces and Interfaces*; Cambridge University Press: Cambridge, UK, 1999.
19. Landel, R. F. *Mechanical Properties of Polymers and Composites*; Marcel Dekker: New York, 1994.
20. Ren, J.; Casanueva, B. F.; Mitchell, C. A.; Krishnamoorti, R. *Macromolecules* 2003, 36, 4188.
21. Krishnamoorti, R.; Yurekli, K. *Curr Opin Colloid Interface Sci* 2001, 6, 464.
22. Galgali, G.; Ramesh, C.; Lele, A. *Macromolecules* 2001, 34, 852.
23. Solomon, M. J.; Almuallam, A. S.; Seefeldt, K. F.; Somwangth-anaroj, A.; Varadan, P. *Macromolecules* 2001, 34, 1864.
24. Vaia, R. A.; Jandt, K. D.; Kramer, E. J.; Giannelis, E. P. *Macromolecules* 1995, 28, 8080.
25. Vaia, R. A.; Jandt, K. D.; Kramer, E. J.; Giannelis, E. P. *Chem Mater* 1996, 8, 2628.